Radiochim. Acta **96**, 823–833 (2008) / **DOI** 10.1524/ract.2008.1528

Pertechnetate immobilization with amorphous iron sulfide

By Y. Liu[1], J. Terry[2] and S. Jurisson[1,*]

[1] Department of Chemistry, University of Missouri-Columbia, Columbia, MO 65211, USA
[2] Department of Biological, Chemical, and Physical Sciences, Illinois Institute of Technology, Chicago, IL 60616, USA

(Received September 12, 2007; accepted in revised form May 27, 2008)

Technetium-99 / Iron sulfide / Pertechnetate immobilization

Summary. The reduction of pertechnetate (TcO_4^-) with freshly prepared amorphous iron sulfide was investigated. The amorphous iron sulfide (FeS) was shown to have an elemental composition of $FeS_{0.97}$ for all of the size fractions and a point of zero charge of $pH_{pzc} = 7.4$. Solubility studies of FeS in various buffers indicated that in the pH range 6.1–9.0, the concentrations of dissociated Fe^{2+} and S^{2-} were negligible. The reductive immobilization of TcO_4^- with FeS was shown to be accelerated by increasing ionic strength and strongly pH dependent. At pH values below the pH_{pzc}, the positively charged FeS surface reacted much faster with TcO_4^- and had higher immobilization yields relative to the negatively charged FeS surface at pH values above pH_{pzc}. The TcO_4^--FeS reaction is consistent with a surface mediated reaction through ligand exchange. The TcO_4^--FeS reductive immobilization reaction product was characterized by X-ray absorption near edge spectroscopy (XANES), extended X-ray absorption fine structure (EXAFS), Fourier transform infrared spectroscopy (FT-IR), and energy dispersive X-ray spectroscopy (EDS) and found to be predominantly TcO_2. Studies on the reductive capacity of the FeS and the long term stability of the TcO_4^--FeS reaction product under both anaerobic and aerobic environments shows the potential utility of the *in situ* gaseous (hydrogen sulfide gas) immobilization technology in solidification of TcO_4^- by creating a FeS permeable reaction barrier in the vadose zone.

Introduction

The Department of Energy Hanford Site in eastern Washington State is the largest nuclear waste storage site in the United States, with 54 million gallons of radioactive waste contained underground in storage tanks [1–3]. The first tank leak, reported in 1956, was a result of corrosion, with about 67 tanks believed to have leaked about 0.75–1.5 million gallons of radioactive waste into the soil, resulting in the contamination of the vadose zone [4].

Among the 46 radionuclides in the waste tanks [5], technetium-99 (Tc-99) is of considerable interest due to the quantities present, its long half-life ($t_{1/2} = 2.13 \times 10^5$ years), and its diverse chemistry [6–8]. Various remediation methods for technetium contamination in the vadose zone from tank leakage at the Hanford Site have been considered [9–14]. The gas-phase approach using hydrogen sulfide (H_2S) gas, which is specifically designed for vadose zone treatment, is attractive due to Tc-99 contaminated soil. The relatively easy introduction of the H_2S gas to the vadose zone, the control of H_2S delivery, and the efficient removal of H_2S gas after completion of the treatment all add to the potential utility of the *in situ* H_2S gaseous remediation method to both laboratory and real field applications [15–17].

The concentration of TcO_4^- in the tanks was at the 10^{-5} M level, indicating the TcO_4^- concentration in the vadose zone would be lower than this. Once the H_2S gas, in large excess, is introduced into the vadose zone, the fraction of H_2S that reacts with TcO_4^- and the rate of oxidation of H_2S in the gas phase would be insignificant [2, 18]. As a result, the main pathway for excess H_2S consumption in the vadose zone would involve reactions with minerals.

Iron oxides are the major constitutes of the soil in the vadose zone [19, 20] and they have been reported to effectively remove H_2S from the gas stream through a gas–solid reaction, to a theoretical maximum of 0.6 g H_2S/g Fe-oxide(s) [21]. This indicates that significant amounts of H_2S would be consumed by iron oxides present in the vadose zone during *in situ* gaseous immobilization to generate significant quantities of iron sulfide (FeS) [22, 23]. FeS might also be generated from dissimilatory sulfate reduction by bacteria present in the soil [24, 25] with no difference in the FeS product [26, 27].

Amorphous FeS is a highly reactive phase and has been widely used to reduce mobile non-radioactive metal oxyanions to insoluble species [28–30]. The interaction between iron sulfide and TcO_4^- showed that TcO_4^- in aqueous solution could be effectively reduced and coprecipitated with FeS [31–34], with a TcS_2-like product identified by X-ray absorption spectroscopy [35–37]. Further studies on the reoxidation of the FeS host with aging showed that rather than being oxidized back to TcO_4^-, a TcO_2-like phase formed, indicating that long term immobilization might be achieved [36, 37]. Based on these results, it may be possible to inject H_2S gas into the vadose zone to reduce the iron oxides to FeS, creating a permeable reactive barrier of FeS for preventing the migration of TcO_4^-. However, the FeS-TcO_4^- reaction is not well understood regarding the stoichiometry of the reaction, factors influencing the reaction, the reaction capacity, or the product characterization. The objectives of this study were to (1) study the basic chemistry between FeS and TcO_4^- in aqueous solution under anaer-

*Author for correspondence (E-mail: JurissonS@missouri.edu).

obic environments, including the effects of pH and ionic strength; (2) study the reaction capacity of FeS for TcO_4^- and the stability of the product under both aerobic and anaerobic environments; and (3) characterize the products generated during the TcO_4^--FeS reaction.

Experimental section

Materials

Caution! Tc-99 is a weak β-emitter ($E_{max} = 294$ keV, 100%). All operations were carried out in a radiochemical laboratory equipped for handling this radionuclide. Solid ammonium pertechnetate was obtained from Oak Ridge National Laboratory. This material, which should be white, was black indicating it had undergone radiolytic autoreduction to TcO_2. Pertechnetate was regenerated by refluxing this mostly black solid with hydrogen peroxide for 1 h.

All water used was 18-MΩ water (Barnstead, USA). Except where noted, chemicals were reagent grade, obtained from either Aldrich Chemical Co. or Fisher Scientific, and used without further purification. Anaerobic studies were done at room temperature in an inert glove box filled with argon. A NaCl solution (0.1 M) was used for ionic strength control except where indicated, as it did not react with any reagents or products. All solutions used in the anaerobic studies were freshly prepared with 18-MΩ water that had been purged with Ar for 2 h prior to use. The aerobic studies were carried out on a laboratory bench with freshly prepared solutions that had not been degassed and were open to the atmosphere. All sample preparations were done in 10 mL sterile vials following the sequence: 5.0 mL of 0.1 M NaCl solution, FeS solid (0.75–15.0 mg), equilibration for 10 min, and finally the TcO_4^- solution. Controls, which were identical to the samples except for the absence of FeS, were run simultaneously under the same conditions. After preparation, the vial was immediately capped with a teflon-lined septum, crimp-sealed with an aluminum cap, evacuated by syringe and flushed 5 times with Ar. All samples were stirred with teflon coated stir bars and run in quadruplicate ($n = 4$).

FeS preparation

A stock amorphous iron sulfide (FeS) suspension was prepared by mixing equal volumes (20 mL) of 1.0 M $Fe(NH_4)_2(SO_4)_2$ and 1.0 M Na_2S solutions at a constant rate of 0.5 L/min into a 2.0 L reaction vessel while stirring at 800 rpm under Ar [38]. The suspension was filtered using a 0.2 μm nylon filter to isolate the solid, which was then freeze-dried in a lyophilizer over 3–4 days. Following lyophilization, the FeS was sealed in a 10 mL vial filled with Ar and stored at −18 °C until use.

Potentiometric titrations

Potentiometric titrations were used to measure the point of zero charge (pH_{pzc}) of the FeS [38, 39]. Due to the sensitivity of the sulfide surface to oxidation by oxygen [40, 41], all potentiometric titrations were done manually under anaerobic environments. The FeS titrations were conducted on an *in situ* precipitated FeS suspension in 0.1 M NaCl solution. The suspension was filtered through a 0.2 μm nylon filter, washed with pure water and then returned to the titration vessel containing background electrolyte solution (*i.e.*, 0.01, 0.1 and 1.0 M NaCl). The titrations were performed at room temperature from pH 6 to pH 10.5 with 0.1 M HCl and 0.1 M NaOH following the procedures reported by Parks *et al.* [42].

Solubility of FeS

The solubility of FeS was determined in 0.1 M NaCl solution, pure water, 0.1 M PIPES (1,4-piperazinebis(ethanesulfonic acid), $pK_a = 6.80$ at 20 °C) buffer (pH 6.1 and 7.0), 0.1 M HEPES (2-[4-(2-hydroxyethyl)-1-piperazine]ethanesulfonic acid, $pK_a = 7.55$ at 20 °C) buffer (pH 7.4), and 0.1 M Tris-HCl (tris(hydroxyl-methyl)aminomethane, $pK_a = 8.3$ at 20 °C) buffer (pH 8.5 and 9.0) under anaerobic conditions. Freshly prepared FeS (5.0 mg) was stirred with a teflon coated magnetic stirrer in 50 mL of fully degassed solution under anaerobic conditions. The samples were collected immediately following equilibration of FeS in the solutions and 24 h later. Since some of the FeS particles were in the nanometer size range and would not be removed by the 0.2 μm nylon filter, all the samples were kept sealed and centrifuged for at least 10 min prior to analysis. The supernatant was filtered and used for UV-vis measurements for sulfide, Fe^{3+} and Fe^{2+} (Ocean Optics USB2000 Spectrometer) [43, 44].

Product stability, reaction stoichiometry, and reaction capacity

The stability of the products obtained from the FeS-TcO_4^- reaction was studied under both anaerobic and aerobic environments in 0.1 M NaCl solution over a period of 8 months. The stability of the product was evaluated using the concentration of TcO_4^- found in solution over time using liquid scintillation counting (LSC) and thin layer chromatography for product identification. The results from this study were used to hypothesize the stoichiometry of the reaction between FeS and TcO_4^- and to calculate the immobilization capacity of FeS for TcO_4^-.

Factors influencing the FeS-TcO_4^- reaction

The effect(s) of ionic strength on the FeS-TcO_4^- reaction under anaerobic environments was studied in 0.1, 0.5 and 1.0 M NaCl solution at FeS and TcO_4^- concentrations of 0.15 mg/mL and 150 μM, respectively. The effect(s) of pH was investigated at the same FeS and TcO_4^- concentrations and the same buffers (pH 6.1–9) as used for the FeS solubility study.

Analyses

Transmission electron microscopy (TEM) imaging analysis of freeze-dried FeS was performed on a JEOL 1200EX transmission electron microscope (100 kV) (JEOL, Japan). Scanning electron microscopy (SEM) imaging and energy

dispersive X-ray spectroscopy (EDS) analysis were performed on a Hitachi S4700 field emission scanning electron microscope (5.0 kV) (Hitachi, Japan). The EDS data were used qualitatively. Approximately 1.0 mg of freeze-dried FeS dispersed in acetone was quickly loaded onto a copper grid coated with carbon in a glovebox, dried under vacuum overnight and mounted into a low-background specimen microscope holder. Both TEM and SEM-EDS images were recorded photographically. The electron microscopy analyses were done at the Electron Microscopy Core at the University of Missouri.

The Brunauer, Emmett, and Teller (BET) surface areas (nitrogen gas, 11 point measurement) were measured with a Quantachrome Autosorb 1-C automated gas sorption system (Quantachrome Instruments, USA) in the Chemical and Biological Engineering Department at the University of Missouri-Rolla.

Liquid scintillation counting (LSC) of ^{99}Tc was performed using a Delta 300 liquid scintillation counter, with an efficiency of 98% for Tc-99 (channels 50–950). All samples were centrifuged for 10 min and only the top of the clear supernatant was used for counting. The sample occasionally contained immobilized Tc compounds in colloidal form (*i.e.*, black color visible) that could not be removed by centrifugation; silica gel thin layer chromatography (TLC) analyses with saline and acetone as the developing agents were then used to determine the percentages of colloidal sample and pertechnetate present. The developed TLC plates were analyzed with a Bioscan 200 Imaging Scanner. Fourier transform infrared (FT-IR) spectroscopy studies of the products generated from the TcO_4^--FeS reaction were run with nujol mineral oil and disposable Thermo ST-IR cards composed of microporous polyethylene (PE)/polytetrafluoroethylene (PTFE) substrates on a Thermo Nicolet Magna-IR spectrometer 550. The pH and potential of the solutions were measured with an Accumet 910 pH meter equipped with an Accumet glass pH combination electrode with a single junction calomel reference, which was calibrated with certified pH 4, 7 and 10 buffers.

X-ray absorption spectroscopy (XAS) [45] was used for characterization of solid products obtained from the reactions. The samples were prepared, triply-encapsulated, and sealed in a bag filled with Ar to prevent oxidation of the samples, at the University of Missouri prior to shipment to the Advanced Photon Source (APS, Argonne IL). The Tc *K*-edge (21 044 eV) X-ray absorption spectra were measured at the Material Research Collaborative Access Team (MRCAT) undulator beamline (10-ID-B). Due to a range of Tc concentrations, X-ray absorption spectra were collected in either transmission or fluorescence geometries. Transmission measurements utilized two Boyd Technologies' ion chambers. The incident energy monitor used 100% N_2 as the detection gas, while the transmission chamber used a gas mixture of 75% N_2 : 25% Ar. Fluorescence data were collected with a sixteen-element germanium detector (Canberra Detector with XIA electronics). The beamline used a double-crystal Si(111) monochromator for energy selection and a rhodium mirror for harmonic rejection. The photon energy was calibrated with an off-axis uranium dioxide reference sample using scattered radiation to excite the U L_2-edge (20 955 eV).

The spectra were reduced, according to the standard EXAFS analysis procedures, using the XAMath [46], IFEFFIT [47], Athena [48], and FEFF 8.4 mpi [49] software packages. The spectra were aligned and summed with XAMath. Fitting and reduction was done in IFEFFIT using theoretical standards calculated with FEFF. Linear combination fitting of XANES spectra [50–52] has been demonstrated to be quantitative when applied to environmental problems including work involving Tc [53]. Athena was used to fit the near-edge region of the XAS spectra as a linear combination of reference spectra with typical relative errors on the order of 5%–10%. Recent work suggests that material preparation can affect this error [54, 55]. The XANES reference spectra were collected from both TcO_2 and TcO_4^- standards prepared previously reported [17, 68]. Our reference standards were prepared and mounted as fine powders to minimize XAS measurement errors.

Results and discussion

The interaction between H_2S and Fe-bearing minerals has shown the potential for creating a permeable reactive barrier of FeS in soil that may be useful for immobilizing $^{99}TcO_4^-$ based on reactions reported between FeS and TcO_4^- [22, 23, 28–30]. However, the reductive FeS-TcO_4^- immobilization reaction is not well understood, and particularly not under environmental conditions that are much more complex. Thus, the basic chemistry between FeS and TcO_4^- was investigated, including (1) preparation and characterization of FeS, (2) effects of solubility, pH and ionic strength on the reductive immobilizaiton of $^{99}TcO_4^-$ by FeS, (3) characterization, reaction stoichiometry, and stability of the immobilized ^{99}Tc product, and (4) determination of the reductive capacity of the FeS.

FeS characterization

FeS was freshly prepared, and the freeze-dried FeS was examined by TEM (Fig. 1) and SEM-EDS. The FeS aggregated as micron-sized particles consisting of smaller subparticles and particle clusters. The aggregation may have resulted from filtration and subsequent freeze-drying of the FeS suspension. The subparticles ranged from 20 nm up

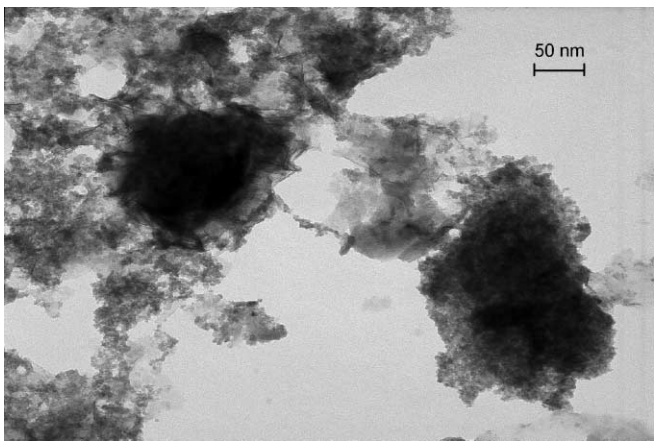

Fig. 1. TEM Image of freeze-dried FeS (100.0 kV × 100 K).

in size, with a highly porous surface. The B.E.T. surface area was measured as 66.96 m^2/g, which is consistent with Wolthers *et al.* [56] The EDS measurements performed on various sized particles showed this FeS yields an approximate Fe : S ratio of 1 ($FeS_{0.97}$), which is consistent for all size fractions and agrees well with Mullet *et al.* [57].

Potentiometric titrations

Potentiometric titrations of the FeS suspensions showed that the three curves for 0.01, 0.1, and 1.0 M NaCl intercept at pH 7.4 (Fig. 2), indicating the pH_{pzc} of this synthetic amorphous FeS is pH 7.4 (± 0.3, $n = 3$). This value is much higher than that reported by Widler ($pH_{pzc} = 2.9$) [58], but consistent with the values reported by Wolthers ($pH_{pzc} = 7.5$) [38]. Thus at pH $>\sim 7.4$, the surface becomes increasingly negatively charged, approaching saturation at high pH, while at pH $<\sim 7.4$, the surface becomes increasingly positively charged until the surface approaches saturation at pH 6.

FeS solubility

Iron sulfide dissolves to some extent in aqueous solution, and Fe^{2+} can reduce TcO_4^- in acidic solution, although the reaction is slow [59]. Our previous studies showed that soluble sulfide immobilizes TcO_4^- in aqueous solution yielding Tc_2S_7, in which the Tc is most likely in the +4 oxidation state [17]. Thus, the concentrations of Fe^{2+} and S^{2-} from dissolution of FeS in the selected pH range were determined.

The results showed that the solution pH (6.1–9.0) was the most important factor for FeS dissolution under anaerobic environments, with increasing dissolution of FeS observed as the pH decreased (data not shown) using previously reported methods [43, 44]. Although extending the stirring time to 24 h increased the dissolved FeS slightly, all the data showed that less than 0.4% of the FeS was dissolved, indicating that the amount of Fe^{2+} dissociated from FeS was negligible in the pH range studied. The concentrations of S^{2-} determined from the dissociation of FeS were also measured and were consistent with the data from the Fe analysis.

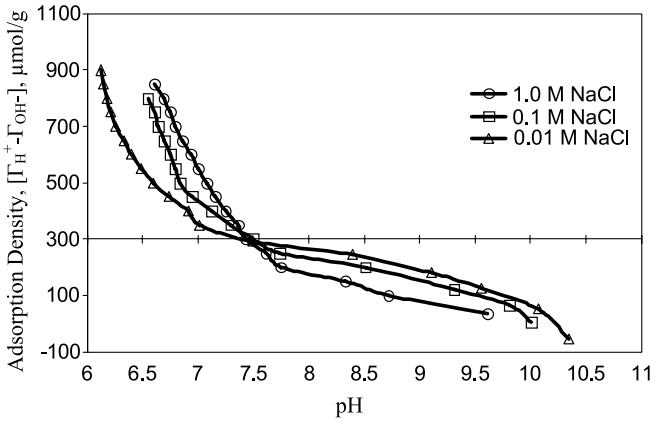

Fig. 2. Adsorption density of the FeS surface as a function of pH and ionic strength (error bars omitted for clarity; all $< 7.7\%$; $n = 3$); the intersection of the curves is the point of zero charge (pH_{pzc}).

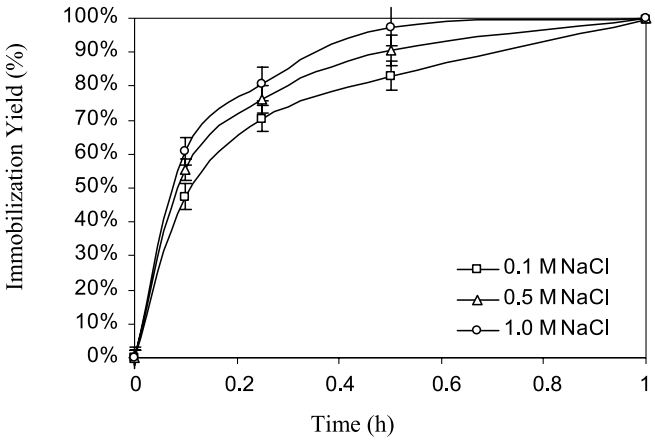

Fig. 3. Effect of ionic strength on the reductive immobilization of TcO_4^- by FeS under anaerobic conditions; TcO_4^-: 150 μM; FeS: 0.15 mg/mL ($n = 4$).

Ionic strength effects on the immobilization of TcO_4^- with FeS

The effects of ionic strength on the reduction of TcO_4^- by Fe(II)-bearing minerals have been reported and the reduction rate of TcO_4^- increased with increasing ionic strength [60–62]. In this study, the influence of ionic strength on the reduction of TcO_4^- (150 μM) by FeS (0.15 mg/mL) in pH 6.5 NaCl solution (0.1–1.0 M) under anaerobic environments is shown in Fig. 3. The reaction of TcO_4^- with FeS was accelerated at higher ionic strengths (Fig. 3), however, the differences in rate were not very large at the ionic strengths investigated because all of the reactions were very fast; this is consistent with other studies [60–62]. In 1.0 M NaCl, the yield was 13.5% higher than that in 0.1 M NaCl (60.8% *vs.* 47.3% at 0.1 h). The effect of ionic strength (0.1 M–1.0 M NaCl) on the TcO_4^--FeS reaction was also studied with higher concentrations of TcO_4^- (2000 μM) and FeS (1.0 mg/mL), with similar results (data not shown).

Effects of pH on the immobilization of TcO_4^- by FeS

The pH-dependence of the reduction of oxyanions by Fe(II)-containing materials such as $Fe(OH)_2$ has been extensively studied [60, 63]. Cui *et al.* [60] demonstrated a linear decrease in the rate of TcO_4^- reduction with increasing pH by more than 1 order of magnitude in the pH range of 7–9.5. In this study, the effects of pH on the reaction of TcO_4^- (150 μM) with synthetic FeS (0.15 mg/mL) were studied under anaerobic environments with 0.1 M buffer in the pH range of 6.1 to 9.0.

Fig. 4 shows the TcO_4^--FeS reaction is strongly pH-dependent, with both the reaction rate and the immobilization yield decreasing sharply with increasing pH. At 0.25 h (Fig. 4), the immobilization yields at pH 6.1 and 7.0 were one order of magnitude higher than those observed at pH 8.5 and 9.0. A similar pH effect was observed at higher TcO_4^- and FeS concentrations (2000 μM and 1.0 mg/mL, respectively) (data not shown).

The reduction of TcO_4^- in solution by Fe(II)-bearing minerals has been reported to proceed *via* heterogeneous electron transfer from structurally bound Fe(II) and involves

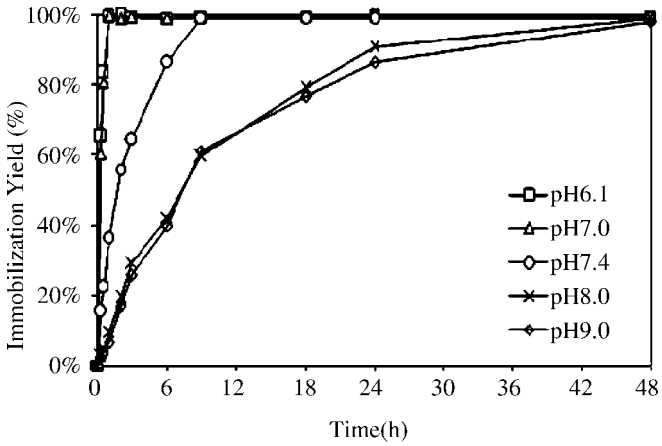

Fig. 4. Effect of pH on the reductive immobilization of TcO_4^- by FeS under anaerobic conditions; TcO_4^-: 150 μM; FeS: 0.15 mg/mL; ionic strength: 0.1 M ($n = 4$).

several steps such as the sorption of TcO_4^- on the surface of the minerals, electron transfer between the solid interface and the adsorbed oxidant, solid state electrochemical reactions and electron transfer [60]. The sorption of TcO_4^- on the surface was reported to be the rate determining step. Thus, a ligand exchange reaction was proposed to explain the sorption of TcO_4^- on the surface of Fe(II)-bearing minerals [60]. The TcO_4^--FeS reaction reported here also showed similar ionic strength effects and pH-dependence, indicating that the sorption of TcO_4^- on the FeS surface may also follow a ligand exchange process [60].

FeS surfaces are reported to have two possible functional groups: a ferrous hydroxyl group, $-FeOH^0$, and a ferrous mercapto group, $-FeSH^0$ [40, 64]. According to Wolthers *et al.* [38], the Fe–SH bond is favored below pH ∼ 10. FeSH sites thus dominate over –FeOH sites on the hydrated FeS surface below pH 10, and can be described as mono-coordinated (FeSH) and tri-coordinated sulfur (Fe_3SH) sites. As our preparation of FeS followed the procedure of Wolthers [38], the asymmetry of the surface charge curves shown in Fig. 2 indicates the presence of these sites.

The surface charge of solids in solution is strongly affected by pH [65]. When the pH of a solution is lower than pH_{pzc}, both the mono-coordinated and tri-coordinated sulfur sites will protonate and the surface of FeS will be positively charged, while at pH higher than pH_{pzc}, the FeS surface will be negatively charged.

The reductive adsorption of TcO_4^- on the surface of magnetite (Fe_3O_4) was viewed as proceeding *via* a positive electrostatic attraction by the magnetite surface for TcO_4^- at pH values below pH_{pzc} [66]. Applying this proposed model and the sorption mechanism to our study, the FeS surface is composed of positively charged $FeSH_2^+$ and $Fe_3SH_2^+$ sites below pH_{pzc}, and the negatively charged TcO_4^- will be attracted to these sites by electrostatic interactions accelerating the ligand exchange rate. The results support this with fast reaction rates observed at pH 6.1 and pH 7.0 (Fig. 4). At pH 8.5 and 9.0, the negatively charged FeS^- and Fe_3S^- sites repel the approaching TcO_4^- and the reductive immobilization reaction is retarded (Fig. 4). Although the immobilization yields for pH 8.5 and pH 9 samples are less than 20% at 2 h (Fig. 4) due to retardation, all of the TcO_4^- is reduced by 48 h, consistent with the hypothesis. In addition, the EXAFS characterization of the product generated indicated no Tc–Fe bond, suggesting an outer-sphere complexation that probably involves electrostatic interactions [65, 67].

Sample characterization

X-ray absorption spectroscopy (XAS) was used to characterize the black precipitates generated in the TcO_4^--FeS reactions in 0.1 M NaCl solution under anaerobic environments. Three samples with immobilization yields of about 30, 60 and 100% were prepared by using different quantities of FeS (1.0, 2.0 and 10.0 mg, respectively). These XAS measurements were compared to reference spectra collected on TcO_4^- and $TcO_2 \cdot nH_2O$ standards prepared as previously described [17, 68].

Fig. 5 shows the near-edge (XANES) region of the Tc *K*-edge X-ray absorption spectra from the samples obtained from the TcO_4^--FeS reductive immobilization reactions and both the TcO_2 and TcO_4^- reference standards. Tc *K*-edge XANES positions have been shown to be less highly correlated with oxidation state than other materials [69, 70]. However, the distinct spectral line-shapes have provided "fingerprint" regions that are useful for compound determination. Table 1 gives the pre-edge peak position, derivative position and maximum photon energies determined from these spectra. The three samples had identical edge positions to that of the TcO_2 standard (21 058 eV) based on the derivative position. The pertechnetate spectrum has an intense pre-edge feature at 21 048.5 eV, while the TcO_2 standard does not [17]. The pertechneate pre-edge "fingerprint" was not observed in the spectra from the three samples, indicating that pertechnetate was not present in the reaction products. Qualitative analysis of the XANES data indicates that the reaction products have been reduced to TcO_2 from the starting material TcO_4^-. Quantitative, linear combination fitting (not shown here) with the two standards indicated that the spectra from the three samples were > 95% TcO_2.

We performed calculations based on the TcO_2 structure [71] and the TcO_4^- structure [72] using FEFF 8.4 mpi [49]

Table 1. Tc *K*-edge XANES parameters from spectra in Fig. 5.

Spectrum	Pre-edge peak (keV)	Derivative position (keV)	Maximum (keV)
TcO_4^-	21.0485	21.062	21.090
TcO_2	21.049	21.058	21.081
TcO_4^--FeS 30% yield	21.049	21.058	21.081
TcO_4^--FeS 60% yield	21.049	21.058	21.081
TcO_4^--FeS 100% yield	21.049	21.058	21.081

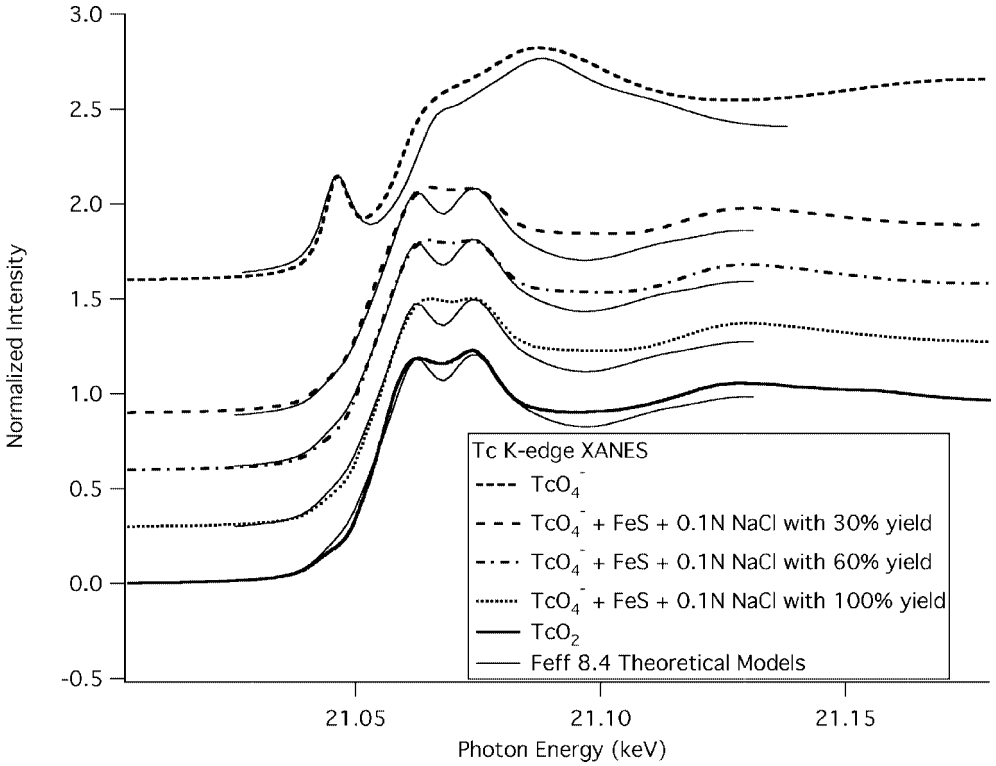

Fig. 5. Tc *K*-edge XANES spectra from TcO_2, TcO_4^-, and three FeS exposed samples. The best theoretical calculations using TcO_4^- and TcO_2 crystal structures are shown for each compound.

to simulate the XANES region of the standards. The use of FEFF in the simulation of XANES spectra has been described in detail elsewhere [49]. The calculations described here assumed the presence of a core hole, allowed quadrupole transitions, and were set up for solid state rather than molecular calculations. Fig. 5 shows the calculated XANES spectra compared to the experimental data. The calculation of the pertechnetate reproduces the intense pre-edge and the wide bandwidth (60 eV) with the two peaks in the XANES region. The dioxide calculations reproduce the narrow bandwith (40 eV), twin humps in the XANES region and show the absence of a major pre-edge feature. The calculated spectrum from the TcO_2 has also been overlayed with the experimental data from the three samples. This calculation matches both the bandwidth and the spectral shape of the experimental XANES spectra from the three samples. While it is not currently possible to calculate "line on line" matches [73] between theoretical and experimental XANES spectra with current *ab initio* XANES methodologies, our calculated spectra clearly show that the reduction products are predominantly TcO_2.

Qualitative, quantitative, and theoretical analysis of the XANES spectra for the three samples shows that the product of the pertechnetate-FeS reaction was predominantly TcO_2. This was confirmed by fitting the extended X-ray absorption fine structure data (EXAFS) from these samples.

Extended X-ray absorption fine structure data was also collected from the samples. The $\chi(R)$ transformations of the $k^2\chi(k)$ from the TcO_2 standard and the 100% yield sample along with the best fits to the data are shown in Fig. 6. The three reaction products were similar to the TcO_2 standard, so only the fitting parameters from the 100% yield sample

Table 2. Tc *K*-edge EXAFS Fitting Parameters from Spectra in Fig. 6.

Spectrum	Neighbor	Number $S_{O^2} = 0.8$	Interatomic spacing (Å)	Debye–Waller factor (Å^2)	E_0 (eV)
TcO_2	O	6 ± 1	1.99 ± 0.02	0.003 ± 0.002	-6 ± 3
	Tc	2 ± 0.5	2.86 ± 0.02	0.008 ± 0.002	-6 ± 3
	Tc–O–O–Tc	22 ± 5	3.43 ± 0.02	0.008 ± 0.002	-6 ± 3
	O	4 ± 2	3.29 ± 0.05	0.003 ± 0.002	-6 ± 3
	Tc	18 ± 7	3.36 ± 0.07	0.02 ± 0.01	-6 ± 3
TcO_4^--FeS 100% yield	O	5 ± 1	2.01 ± 0.02	0.003 ± 0.002	-6 ± 3
	Tc	2 ± 1	2.92 ± 0.02	0.008 ± 0.002	-6 ± 3
	Tc–O–O–Tc	19 ± 5	3.45 ± 0.02	0.004 ± 0.002	-6 ± 3
	O	5 ± 2	3.29 ± 0.05	0.003 ± 0.002	-6 ± 3
	Tc	12 ± 7	3.35 ± 0.07	0.02 ± 0.01	-6 ± 3

The error bars were set by fixing all other variables and finding the delta that resulted in a 50% increase of the *R*-factor of the best fit (TcO_2 *R*-factor = 0.04; 100% yield sample *R*-factor = 0.01).

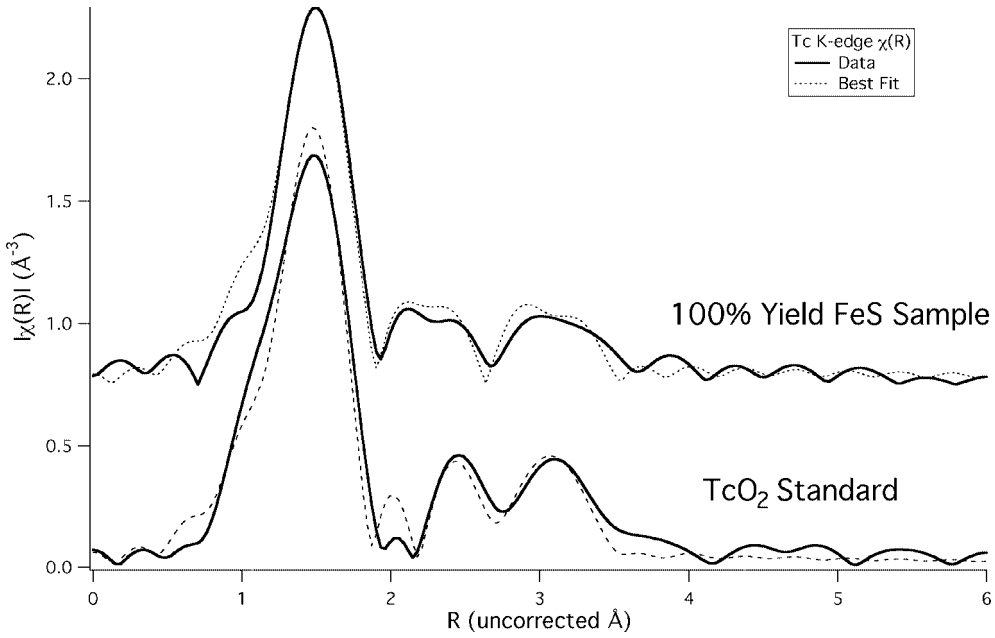

Fig. 6. Tc K-edge $\chi(R)$ function with associated best fits for the 100% yield sample and the TcO_2 standard shown in Fig. 5. The fitting parameters are discussed in the text.

and the standard will be discussed (Table 2). The fitting was performed in positional or R-space over a range from 1.1 to 3.5 Å. The range in momentum or k-space Fourier transformed to give the R-space data was from 2.7 to 10.8 $Å^{-1}$. Simultaneous fitting in R-space was performed using both k^2 and $k^3\chi(k)$ transformations. Focusing on the first three fitting paths that define the local environment around the absorbing Tc atom, we observed that the TcO_2 standard had approximately 6 neighboring O atoms at a distance of 1.99 Å. The standard was found to have 2 neighboring Tc atoms at a distance of 2.86 Å. The third path was a multiple scattering path between the Tc absorber and two neighboring oxygen atoms separated by 90°. This third path clearly shows that the oxygen atoms are in an octahedral arrangement around the Tc absorber. Comparing the standard fit to neutron diffraction data on TcO_2 [71], our EXAFS results are in excellent agreement to the reported average Tc–O bond distance of 1.98 Å with 6 neighbors and the average Tc–Tc bond distance of 2.85 Å with 2 neighbors.

The 100% yield sample was found to have 5 neighboring O atoms at a distance of 2.01 Å and 2 Tc atoms at distance of 2.92 Å. The third multiple scattering path was also very strong in the 100% yield sample, again indicating an octahedral arrangement of the O atoms around the Tc absorber. Overall, the scattering amplitudes were slightly reduced from that of the standard; this may be due to the formation of particles of a smaller size in the reaction product than in the standard sample. It is difficult to extract information for the higher shells due to significant overlap from multiple paths in this region. The EXAFS data was in complete agreement with the XANES results confirming that the samples obtained from the TcO_4^--FeS reductive immobilization reactions with different yields were all predominantly TcO_2.

Haines *et al.* [66] characterized the product obtained from the surface reduction of TcO_4^- with Fe_3O_4 by FT-IR and reported this compound was TcO_2 with a Tc–O stretching vibration band at 896 cm^{-1}. Fig. 7 shows that all three compounds have absorptions at 902 cm^{-1}, consistent with the reported value for the Tc–O stretch in TcO_2, indicating a TcO_2-like compound was produced in the TcO_4^--FeS reaction.

EDS spectra were used to measure the elemental composition on the surface of the product generated from the TcO_4^--FeS reductive immobilization reaction. The absorptions of the S K-edge and the Tc L-edge were measured at 2.30 keV and 2.42 keV, respectively. Fig. 8 clearly showed the presence of Tc on the surface of the product with 60% immobilization yield, although the S and Tc were not well resolved. The at.% concentration of Tc on the product surface was about 5%. For S, the at.% concentration decreased from 30% to ∼ 15%. The at.% concentration of O increased from 10% to ∼ 23%, while the at.% concentration of Fe decreased from 33% to about 20%. It was reported by Livens *et al.* [36, 37] that the product obtained from the TcO_4^--FeS reaction under anaerobic environments was a TcS_2-like compound. If TcS_2 had been generated in the reaction, an increase in the at.% concentration of S should have been observed on the surface of the product. However, a decrease in the at.% concentration for S and Fe was measured along with the increase for Tc. There was no evidence showing the presence of TcS_2 on the surface of the product. This study suggests that TcO_2 is generated during the reaction along with the oxidation of FeS on the surface. The formation of TcO_2 may form a layer on the surface of FeS, resulting in the increases in at.% concentrations of both Tc and O and decreases of both Fe and S observed in the EDS spectra. Although the increase of Tc is not proportional to the increase of O due to the oxidation of FeS to iron oxyhydroxide [28] and the presence of residual water, the EDS spectra clearly show the formation of a TcO_2-like species on the surface generated from the TcO_4^--FeS reductive immobilization reaction.

Stoichiometry study

In an effort to study the stoichiometry between FeS and TcO_4^-, colorimetric methods were used to analyze solution

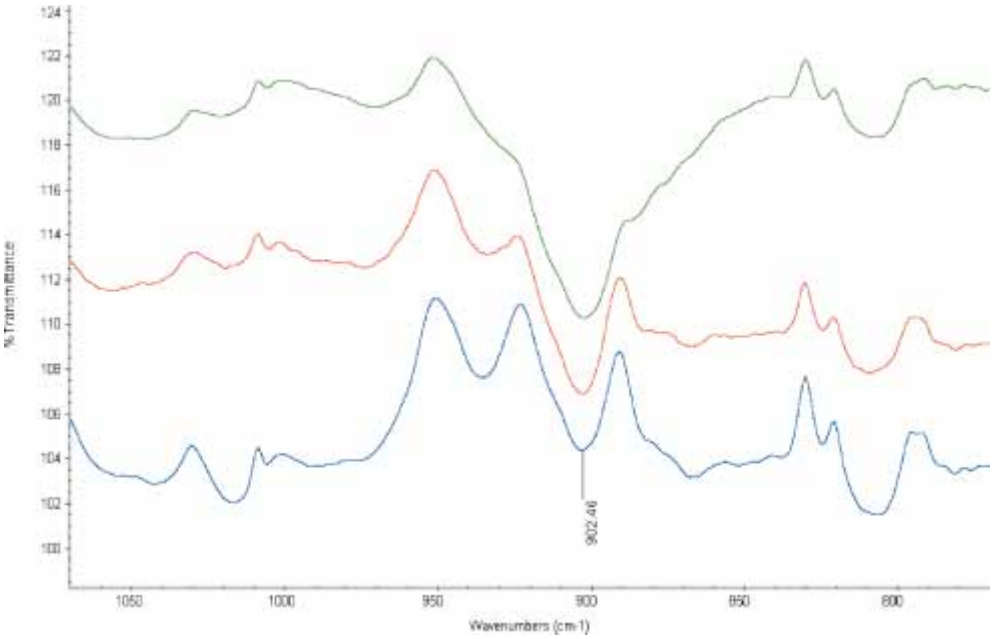

Fig. 7. FT-IR Spectra of the product obtained from the TcO_4^--FeS reaction with 60% yield (bottom), TcO_2 standard in low concentration (middle), TcO_2 standard in high concentration (top).

samples for sulfide [43], Fe^{2+}, Fe^{3+} [44], and other oxidized species of sulfide [74]. The pH of the solution (0.1 M NaCl) was also measured before and after the reaction. The speciation of Fe^{2+} and Fe^{3+} was distinguished by dissolving the product collected from the TcO_4^--FeS reaction with 0.05 M HCl under anaerobic conditions and making the measurements in both the presence and absence of reducing agent.

The spectrophotometric analysis clearly showed the presence of Fe^{3+}, and thiosulfate ($S_2O_3^{2-}$) was the only sulfur species observed. Additionally, the pH of the solution significantly increased during the reaction. Taken together, the solution analysis, product characterization and pH increase suggest the following potential reactions may be occurring

$$10TcO_4^- + 6FeS + 11H_2O \leftrightarrow 10TcO_2 + 6Fe^{3+} + 3S_2O_3^{2-} + 22OH^- \quad (1)$$

or

$$10TcO_4^- + 6FeS + 21H_2O \leftrightarrow 10TcO(OH)_2 + 6Fe^{3+} + 3S_2O_3^{2-} + 22OH^- . \quad (2)$$

Product stability

The reoxidation of the surface reduced product from TcO_4^- solution with Fe(II)-bearing minerals has been reported to be a very slow process [60, 66]. In the absence of other oxidizing agents, TcO_2 will be oxidized to TcO_4^- by the oxygen when exposed to the atmosphere. In this study, the stability of the product generated from the TcO_4^--FeS reaction with about 60% immobilization yield (40% unreacted TcO_4^- and some unreacted FeS remaining in solution) was evaluated under both aerobic and anaerobic environments in 0.1 M NaCl solution at neutral pH.

Under aerobic environments, the concentration of TcO_4^- increased initially due to the oxidation of TcO_2 by O_2 in the air. At the 30th day, the activity of TcO_4^- arising from oxidized TcO_2 reached a maximum of about 30% (Fig. 9). On further reaction, the concentration of TcO_4^- in solution under aerobic environments slowly decreased to about 5% after 50 days with a very slow continued decrease for the following 150 days. A plausible explanation for this behavior is the sorption of TcO_4^- on the oxidized surface of FeS, reported to be iron oxyhydroxide [28]. The hydrous iron oxyhydroxide has the potential to form surface complexes with anions [75] and was reported to have little sorption of TcO_4^- over short time periods (0.24% in 4 h) [76]. However, it is possible that the iron oxyhydroxide sorbed TcO_4^- over a longer period of time, resulting in the decrease of TcO_4^- observed. Additionally, the radiolytic reduction of TcO_4^- to TcO_2 may also contribute to the decrease observed.

Under anaerobic environments, the TcO_4^- concentration in solution decreased over time, presumably from diffusion

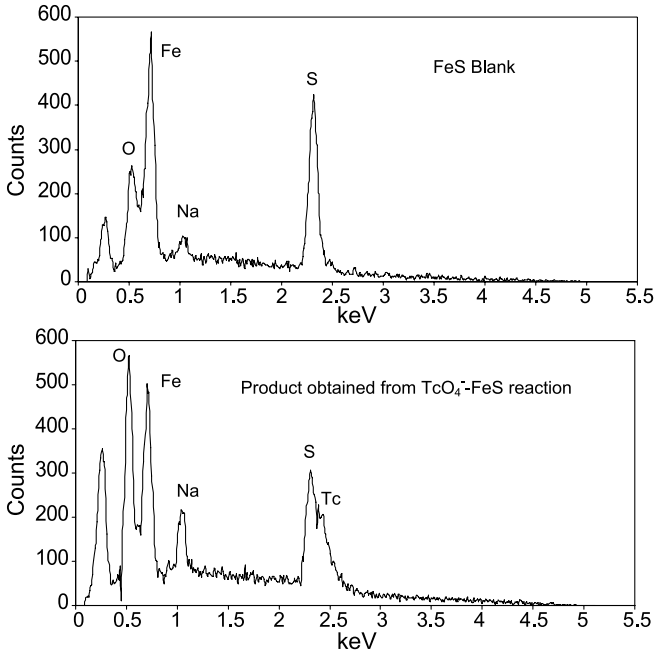

Fig. 8. EDS Spectra of the FeS blank and the product from the TcO_4^--FeS reaction.

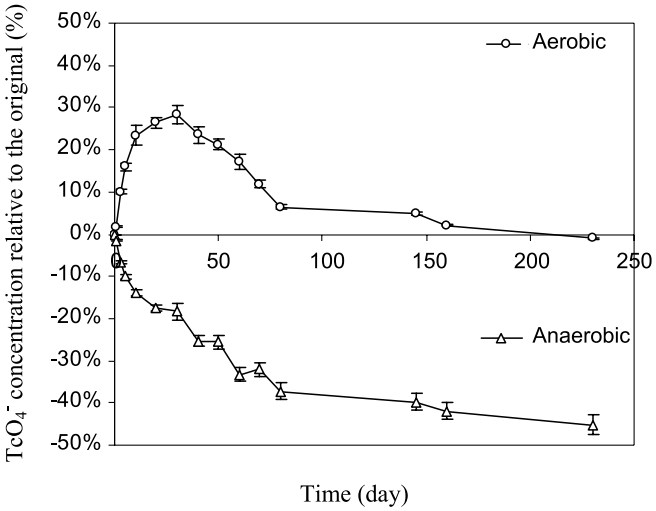

Fig. 9. Stability study of the product formed in TcO_4^--FeS reaction under both aerobic and anaerobic environments.

into the FeS matrix. The rate of TcO_4^- removal from solution gradually slowed, probably due to the increasing difficulty of TcO_4^- diffusion into the reactive sites on the FeS surface.

Reductive capacity of FeS

The reductive capacity of a reductant is an important factor for evaluating its potential for use with *in situ* reduction processes. It can be defined as the amount of an oxidant that can be reduced when sufficient time is given for the reaction to proceed to its maximum extent [77].

The reductive capacity of synthetic iron sulfide for Cr(VI) was reported as 238 mg Cr(VI)/g FeS [29]. In this study, the reductive capacity of the FeS for TcO_4^- was calculated as 867 mg TcO_4^-/g FeS from the stability data from day 160 (Fig. 9), indicating a high potential for application to TcO_4^- immobilization.

Conclusions

The reductive immobilization of TcO_4^- in aqueous solution with synthetic amorphous FeS under anaerobic environments showed a high reductive capacity. The reaction between FeS and TcO_4^- is pH dependent and is accelerated with increasing ionic strength. The reaction is assumed to be surface mediated through a ligand exchange mechanism to generate an outer-sphere complex according to the model of Wolthers [38]. Characterization of the product generated from the TcO_4^--FeS reaction showed it to be TcO_2, which exhibited good stability under anaerobic environments. The long term stability studies (Fig. 9) suggest that FeS has the potential to immobilize TcO_4^- in both anaerobic and aerobic environments and the potential for *in situ* immobilization of TcO_4^- in the vadose zone by H_2S gas when iron-containing minerals are present.

Acknowledgment. This research was supported by the Office of Science (BER), U.U. Department of Energy, Grant No. DE-FG02-03ER63616. Use of the Advanced Photon Source was supported by the U.S. Department of Energy, Office of Science, Office of Basic Energy Sciences, under Contract No. W-31-109-Eng-38. All operations at the Materials Research Collaborative Access Team's Sector 10-ID-B line are funded by contributions from the member institutions. We thank Professor Baolin Deng at University of Missouri-Columbia and Dr. Edward C. Thornton at Pacific Northwest National Laboratory for their valuable support and comments on this work. We thank the assistance of the University of Missouri-Columbia's Electron Microscopy Core Facility for preparing and imaging specimens for this research. We thank the assistance of the Department of Chemical and Biological Engineering of University of Missouri-Rolla for the measurements of surface area.

References

1. Gephart, R. E., Lundgren, R. E.: *Hanford Tank Cleanup: A Guide to Understanding the Technical Issues*. Battelle Press, Columbus, OH (1998).
2. Schroeder, N. C., Radzinski, S. D., Ashley, K. R., Truong, A. P., Whitener, G. D.: Feed adjustment chemistry for Hanford 101-SY and 103-SY tank waste: Attempts to oxidize the non-pertechnetate species. J. Radioanal. Nucl. Chem. **250**, 271 (2001).
3. Lukens, W. W., Shuh, K. D., Schroeder, N. C., Ashley K. R.: Identification of the non-pertechnetate species in Hanford waste tanks, Tc(I)-carbonyl complexes. Environ. Sci. Technol. **38**, 229 (2004).
4. U.S. Department of Energy (DOE). History of the Plutonium Production Facilities at The Hanford Site Historic District, 1943–1990: Richland, Washington: U.S. Department of Energy. DOE/RL-97-1947. Available at http://www.Hanford.gov/docs/rl-97-1047/index-htm, accessed March 2, 2001.
5. Agnew, S. F.: Hanford Tank Chemical and Radionuclide Inventories: HDW Model Rev 4., LA-UR-96-3860, Los Alamos National Laboratory, Los Alamos, NM (1996).
6. Colby, S., Peterson, C.: Inventory of Technetium-99 from Reprocessing Hanford Spent Nuclear Fuel. Westinghouse Hanford Co. Letter Report prepared for the U.S. Department of Energy Office of Environmental Restoration and Waste Management, Richland, WA (1995).
7. Peacock, R. D.: *The Chemistry of Technetium and Rhenium*. Elsevier, New York (1966), pp. 1–78.
8. Rard, J. A.: Critical Review of Chemistry and Thermodynamics of Technetium and Some of Its Inorganic Compounds and Aqueous Species, Lawrence Livermore National Laboratory report UCRL-53440, Livermore, CA (1983), pp. 24–67.
9. Burgeson, I. E., Deschane, J. R., Blanchard Jr., D. L.: Removal of Technetium from Hanford tank waste supernates. Sep. Sci. Technol. **40**, 201 (2005).
10. King, W. D., Hassan, N. M., McCabe, D. J., Hamm, L. L., Johnson, M. E. Technetium removal from Hanford and Savannah River site actual tank waste supernates with Superlig® 639 Resin. Sep. Sci. Technol. **38**, 3093 (2003).
11. Shen, D., Fan, X. H., Su, X. G., Zeng, J. S., Dong, Y.: Sorption of radioactive technetium on pyrrhotine. J. Radioanal. Nucl. Chem. **254**, 137 (2002).
12. Medvedeva, I. B., Kuznetsova, N. A., Rovnyi, S. I.: Tc(VII) sorption by fibrous sorbents. At. Energ. **94**, 318 (2003).
13. Bock, W. D., Brühl, H., Trapp, C., Winkler A.: Sorption properties of natural sulfides with respect to technetium. Mater. Res. Soc. Symp. Proc. **127**, 973 (1989).
14. Mattigod, S. V., Serne, R. J., Fryxell, G. E.: Selection and Testing of "Getters" for Adsorption of Iodine-129 and Technetium-99: A Review. PNNL-14208, Pacific Northwest National Laboratory, Richland, WAq (2003).
15. Thornton, E. C., Amonette, J. E.: Hydrogen sulfide gas treatment of Cr(VI)-contaminated sediment samples from a plating-waste disposal site-implications for *in situ* remediation. Environ. Sci. Technol. **33**, 4096 (1999).
16. Thornton, E. C., Giblin, J. T., Gilmore, T. J., Olsen, K., Phelan, J. M., Miller, R. D.: *In situ* Gaseous Reduction Pilot Demonstration-Final Report, PNNL-12121, Pacific Northwest National Laboratory, Richland, WA (1999).
17. Liu, Y., Terry, J., Jurisson, S.: Pertechnetate immobilization in aqueous media with hydrogen sulfide under anaerobic and aerobic environments. Radiochim. Acta **95**, 717 (2007).
18. Manahan, S. E.: *Fundamental of Environmental Chemistry*. Lewis Publishers, Chelsea, MI (1993).

19. Schwertmann, U.: Solubility and dissolution of iron oxides. Plant Soil **130**, 1 (1991).
20. Lindenmeier, C. W., Lindberg, M. J., Geiszler, K. N., Serne, R. J., Clayton, R. E., Brown, C. F., Bjornstad, B. N., LeGore, V. L., Valenta, M. M., Gee, G. W., Kutnyakor, I. V., Vickerman, T. S., Schaef, H. T., Baum, S. R., Royack, L. J., Lanigan, D. C.: Characterization of Vadose Zone Sediment: RCRA Borehole 299-E33-338 Located Near the B-BX-BY Waste Management Area. PNNL-14121, Pacific Northwest National Laboratory, Richland, WA, June (2003).
21. Kohl, A. L., Riesefedl, F. S.: *Gas Purification*. Gulf, Houston (1985), Chap. 4.
22. Cantrell, K. J., Yabusaki, S. B., Engelhard, M. H., Mitroshkov, A. V., Thornton, E. C.: Oxidation of H_2S by iron oxides in unsaturated conditions. Environ. Sci. Tech. **37**, 2192 (2003).
23. Davydov, A., Chuang, K. T., Sanger, A. R.: Mechanism of H_2S oxidation by ferric oxide and hydroxide surfaces. J. Phys. Chem. B **102**, 4745 (1998).
24. Ivarson, K. C., Hallberg, R. O.: Formation of mackinawite by the microbial reduction of jarosite and its application to tidal sediments. Geoderma **16**, 1 (1976).
25. Watson, J. H. P., Croudace, I. W., Warwick, P. E., James, P. A. B., Charnock, J. M., Ellwood, D. C.: Adsorption of radioactive metals by strongly magnetic iron sulfide nanoparticles produced by sulfate-reducing bacteria. Sep. Sci. Technol. **36**, 2571 (2001).
26. Rickard, D. T.: The Geological and Microbiological Formation of Iron Sulfides. Ph.D. Thesis, London University (1968), p. 283.
27. Rickard, D. T.: The microbiological formation of iron sulfides. Acta Univ. Stockh. **20**, 49 (1969)
28. Patterson, R. R., Fendorf, S.: Reduction of hexavalent chromium by amorphous iron sulfide. Environ. Sci. Technol. **31**, 2039 (1997).
29. Erdem, M., Altundogan, H. S., Özer, A., Tümen, F.: Cr(VI) Reduction in aqueous solutions by using synthetic iron sulphide. Environ. Sci. Technol. **22**, 1213 (2001).
30. Wolthers, M., Charlet, L., Van der Weijden, C. H., Van der Linde, P. R., Rickard, D.: Arsenic mobility in the ambient sulfidic environments: sorption of arsenic(V) and arsenic(III) onto disordered mackinawite. Geochim. Cosmochim. Acta **69**, 3483 (2005).
31. Kunze, S., Neck, V., Gompper, K., Fanghaenel, Th.: Studied on the immobilization of technetium under near field geochemical conditions. Radiochim. Acta **74**, 159 (1996).
32. Lee, S. Y., Bondietti, E. A.: Technetium behavior in sulfide and ferrous iron solutions. Mater. Res. Soc. Symp. Proc. **15**, 315 (1983).
33. Langton C. A.: Slag-Based Materials for Toxic Metal and Radioactive Waste Stabilization. DP-MS-87-95-Rev. 2. E.I. du Pont de Nemours & Co., Savannah River Laboratory, Aiken, SC (1989).
34. Gilliam T. M., Spence, R. D., Bostick, W. D., Shoemaker, J. L.: Solidification/stabilization of technetium in cement-based grouts. J. Hazard. Mater. **24**, 189 (1990).
35. Allen, P. G., Siemering, G. S., Shuh, D. K., Bucher, J. J., Edelstein, N. M., Langton, C. A., Clark, S. B., Reich, T., Denecke, M. A.: Technetium speciation in cement waste forms determined by X-ray absorption fine structure spectroscopy. Radiochim. Acta **76**, 77 (1997).
36. Wharton, M. J., Atkins, B., Charnock, J. M., Livens, F. R., Pattrick, R. A. D., Collison, D.: An X-ray absorption spectroscopy study of the coprecipitation of Tc and Re with mackinawite (FeS). Appl. Geochem. **15**, 347 (2000).
37. Livens, F. R., Jones, M. J., Hynes, A. J., Charnock, J. M., Mosselmans, J. F. W., Hennig, C., Steele, H., Collison, D., Vaughan, D. J., Pattrick, R. A. D., Reed, W. A., Moyes, L. N.: X-ray absorption spectroscopy studies of reactions of technetium, uranium and neptunium with mackinawite. J. Environ. Radioact. **74**, 211 (2004).
38. Wolthers, M., Charlet, L., Van der Linde, P. R., Rickard, D., Van der Weijden, C. H.: Surface chemistry of disordered mackinawite (FeS). Geochim. Cosmochim. Acta **69**, 3469 (2005).
39. Wilder, A. M., Seward, T. M.: The adsorption of gold(I) hydrosulphide complexes by iron sulfide surfaces. Geochim. Cosmochim. Acta **66**, 383 (2002).
40. Bebié, J., Schoonen, M. A. A., Fuhrmann, M., Strongin, D. R.: Surface charge development on transition metal sulfides: an electrokinetic study. Geochim. Cosmochim. Acta **62**, 633 (1998).
41. Fornasiero, D., Eijt, C., Ralston, J.: An electrokinetic study of pyrite oxidation. Colloid Surf. **62**, 63 (1992).
42. Parks, G. A., De Bruyn, P. L.: The zero point of charge of oxides. J. Phys. Chem. **66**, 967 (1962).
43. APHA, AWWA, WPCF. *Standard Methods for the Examination of Water and Wastewater*. 18th Ed., Washington (1992).
44. Gibbs, M. M.: A Simple method for the rapid determination of iron in natural waters. Water Res. **13**, 295 (1979).
45. Koningsberger, D. C., Prins, R.: *X-ray Absorption: Principles, Applications, Techniques of EXAFS, SEXAFS, and XANES*. John Wiley & Sons, New York (1988), p. 673.
46. Wasserman, S.: http://ixs.csrri.iit.edu/database/programs/.
47. Newville, M.: IFEFFIT: Interactive XAFS analysis and FEFF fitting. J. Synchrotron. Radiat. **8**, 322 (2001)
48. Ravel, B., Newville, M.: ATHENA, ARTEMIS, HEPHAESTUS: Data analysis for X-ray absorption spectroscopy using IFEFFIT. J. Synchrotron. Radiat. **12**, 537 (2005).
49. Ankudinov, A. L, Nesvizhskii, A. I., Rehr, J. J.: Dynamic screening effects in X-ray absorption spectra. Phys. Rev. B **67**, 115 (2003).
50. Ressler, T., Wong, J., Roos, J., Smith, I. L.: Quantitative speciation of Mn-bearing particulates emitted from autos burning (methylcyclopentadienyl)manganese tricarbonyl-added gasolines using XANES spectroscopy. Environ. Sci. Technol. **34**, 950 (2000).
51. Pickering, I. F., Brown Jr., G. E., Tokunaga, T. K.: Quantitative speciation of selenium in solils using X-ray absorption spectroscopy. Environ. Sci. Technol. **29**, 2456 (1995).
52. Schilling, P. J., Tittsworth, R. C.: Extraction of phase fractions and compositions for bcc/fcc two-phase binary alloys from XANES data. J. Synchrotron. Radiat. **6**, 497 (1990).
53. Lukens, W. W., Bucher, J. J., Shuh, D. K., Edelstein, N. M.: Evolution of technetium speciation in reducing grout. Environ. Sci. Technol. **39**, 8064 (2005).
54. Ajiboye, B., Akinremi, O. O., Jurgensen, A.: Experimental Validation of quantitative XANES analysis for phosphorous speciation. Soil Sci. Soc. Am. J. **71**, 1288 (2007).
55. Bunker, G.: unpublished data.
56. Wolthers, M., Van der Gasst, S. J., Rickard, D.: The structure of disordered mackinawite. Am. Mineral. **88**, 2007 (2003).
57. Mullet, M., Boursiquot, S., Abdelmoula, M., Génin, J. M., Ehrhardt, J. J.: Surface chemistry and structural properties of mackinawite prepared by reaction of sulfide ions with metallic iron. Geochim. Cosmochim. Acta **66**, 829 (2002).
58. Widler, A. M.: The Adsorption of Gold(I) Hydrosulphide Complexes by Iron Sulphides. Ph.D. Dissertation, Swiss Federal Institute of Technology Zürich (ETHZ), Swiss, December (1999).
59. Cui, D., Eriksen, T. E.: Reduction of pertechnetate by ferrous iron in solution: influence of sorbed and precipitated Fe(II). Environ. Sci. Technol. **30**, 2259 (1996).
60. Cui, D., Eriksen, T. E.: Reduction of pertechnetate in solution by heterogeneous electron transfer from Fe(II)-containing geological material. Environ. Sci. Technol. **30**, 2263 (1996).
61. Vandergraaf, T. T., Ticknor, K. V., George, I. M.: In: *Geological Behavior of Radioactive Waste*. (Barney, G. E., ed.) American Chemical Society Symposium Series 246, American Chemical Society, Washington (1984), p. 24.
62. Byegaard, J., Albinsson, Y., Skarnemark, G., Skaalberg, M.: Field and laboratory studies of the reduction and sorption of technetium(VII). Radiochim. Acta **58/59**, 239 (1992).
63. Aoki, T., Munemori, M.: Reduction of chromium(VI) by iron(II) hydroxide in alkaline solution. Bull. Chem. Soc. Japan **55**, 730 (1982).
64. Kornicker, W. A.: Interactions of divalent cations with pyrite and mackinawite in seawater and sodium-chloride solutions. Ph.D. Thesis, Texas A&M University (1988).
65. Stumm, W., Sigg, L., Sulzberger, B.: *Chemistry of The Solid-Water Interface: Processes at The Mineral-Water and Particle-Water Interface in Natural System*. John Wiley & Sons, New York (1992).

66. Haines, R. I., Owen, D. G., Vandergraaf, T. T.: Technetium-iron oxide reactions under anaerobic conditions: a fourier transform infrared, FTIR study. Nucl. J. Can. **1**, 32 (1987).
67. Hayes, K. F., Roe, A. L., Brown Jr., G. E., Hodgson, K. O., Leckie, J. O., Parks, G. A.: *In situ* X-ray absorption study of surface complexes: selenium oxyanions on α-FeOOH. Science **238**, 783 (1987).
68. Nelson, C. M., Boyd, G. E., Smith Jr., W. T.: Magnetochemistry of technetium and rhenium. J. Am. Chem. Soc. **76**, 348 (1954).
69. Almahamid, I., Bryan, C., Bucher, J. J., Burrell, A. K., Edelstein, N. M., Hudson, E. A., Kaltsoyannis, N., Lukens, W. W., Shuh, D. K., Nitsche, H., Reich, T.: Electronic and structural investigations of technetium compounds by X-ray absorption spectroscopy. Inorg. Chem. **34**, 193 (1995).
70. Terry, J., Grzenia, B., Papagiannopoulou, D., Kyger, J., Jurisson, S., Robertson, J. D.: Structural determination of Tc-99 radiopharmaceuticals and compounds using X-ray absorption spectroscopy. J. Radioanal. Nucl. Chem. **263**, 531 (2005).
71. Rodgriguez, E. E., Poineau, F., Llobet, A., Sattelberger, A. P., Bhattacharjee, J., Waghmare, U. V., Hartmann, T., Cheetham, A. K.: Structural studies of TcO_2 by neutron powder diffraction and first-principles calculations. J. Am. Chem. Soc. **129**, 10 244 (2007).
72. Faggiani, R., Lock, C. J. L., Poce, J.: The structure of ammonium pertechnetate at 295, 208, and 141 K. Acta Cryst. B **36**, 231 (1980).
73. Smolentsev, G., Soldatov, A. V.: FitIt: New software to extract structural information on the basis of XANES fitting. Comput. Mater. Sci. **39**, 569 (2007).
74. Koh, T., Okabe, K.: Spectrophotometric determination of sulfide, sulfite, thiosulfate, trithionate and tetrathionate in mixtures. Analyst **119**, 2457 (1994).
75. Sigg, L., Stumm, W.: The interaction of anions and weak acids with the hydrous goethite (α-FeOOH) surface. Colloid Surf. **2**, 101 (1980).
76. Walton, F. B., Paquette, J., Ross, J. P. M., Lawrence, W. E.: Tc(IV) and Tc(VII) interactions with iron oxyhydroxides. Nucl. Chem. Waste Manag. **6**, 121 (1986).
77. Lee, W. J., Batchelor, B.: Reductive capacity of natural reductants. Environ. Sci. Technol. **37**, 535 (2003).